

## Natural convection in asymmetric triangular enclosures heated from below

O.M. Kamiyo<sup>1</sup>, D. Angeli<sup>2</sup>, G.S. Barozzi<sup>3,\*</sup> and M.W. Collins<sup>4,†</sup>

<sup>1</sup>Department of Mechanical Engineering, University of Lagos, Lagos, Nigeria.

<sup>2</sup>DISMI – Dipartimento di Scienze e Metodi dell'Ingegneria, Università di Modena e Reggio Emilia, via Amendola 2, I-42122 Reggio Emilia, Italy

<sup>3</sup>DIEF - Dipartimento di Ingegneria "Enzo Ferrari", Università di Modena e Reggio Emilia, via Vignolese 905, I-41125 Modena, Italy

<sup>4</sup>School of Engineering and Design, Brunel University, Uxbridge, Middlesex, UB8 3PH, UK

\*E-mail: giovanni.barozzi@unimore.it

†Prof. Michael Wesley Collins passed on 2014 August 24<sup>th</sup>. Among a number of scientific topics he cultivated in his brilliant academic career, convection heat transfer was the first and the most beloved.

**Abstract.** Triangular enclosures are typical configurations of attic spaces found in residential as well as industrial pitched-roof buildings. Natural convection in triangular rooftops has received considerable attention over the years, mainly on right-angled and isosceles enclosures. In this paper, a finite volume CFD package is employed to study the laminar air flow and temperature distribution in asymmetric rooftop-shaped triangular enclosures when heated isothermally from the base wall, for aspect ratios (AR)  $0.2 \leq AR \leq 1.0$ , and Rayleigh number (Ra) values  $8 \times 10^5 \leq Ra \leq 5 \times 10^7$ . The effects of Rayleigh number and pitch angle on the flow structure and temperature distributions within the enclosure are analysed. Results indicate that, at low pitch angle, the heat transfer between the cold inclined and the hot base walls is very high, resulting in a multi-cellular flow structure. As the pitch angle increases, however, the number of cells reduces, and the total heat transfer rate progressively reduces, even if the Rayleigh number, being based on the enclosure height, rapidly increases. Physical reasons for the above effect are inspected.

### 1. Introduction

The study of natural convection in rooftop enclosures is gaining importance for various environmental applications. In roof design, the attic space is often given paramount consideration because its thermal characteristics have great influence on the conditions of the space directly below it. In tropical climates, both humid and arid, conventional types of roof construction suffer from excessive mid-day overheating due to the high solar radiation incident on the surface area. Solar radiation absorption can actually cause the roofing sheets to become very hot in the midday sun. A low-pitched roof, common in the tropics, is particularly prone to trap heat in the attic, and a significant amount of the cooling load in residential and industrial buildings is the result of heat transfer across the ceiling from the attic [1]. Also, in some rural areas, agricultural produce are sometimes kept in the rooftops of residences either



for drying or for storage. It is, therefore, desirable to have a thorough knowledge of the flow patterns and heat transfer characteristics of the attic space under realistic conditions.

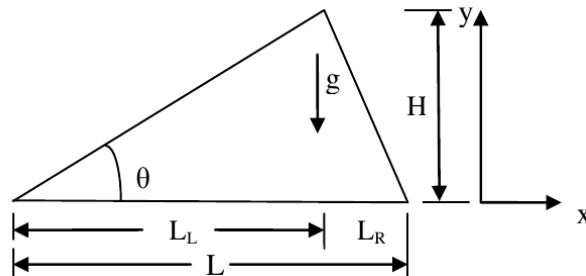


**Figure 1.** Physical Model

Natural convection heat transfer and fluid flow in enclosed spaces has been studied extensively in recent years especially in response to energy-related applications. The earlier numerical study was carried out by Gershuni et al. in 1974 [2]. In their work, they investigated specific features of fluid motion in an enclosure with bottom heating. Studies carried out by Poulikakos and Bejan [3] for a right-triangular enclosure indicate single cell fluid circulations for Rayleigh numbers ( $Ra$ ) up to  $10^4$ , and for values of the aspect ratio ( $AR$ ) between 0.02 and 1.0. Ridouane and Campo [4] observed that, for  $10^2 \leq Ra \leq 10^5$ , the flow bifurcation is time-dependent. Sahar et al. [5] studied natural convection in tilted isosceles triangular enclosures with discrete bottom heating for  $10^3 \leq Gr \leq 10^6$ ,  $0.5 \leq AR \leq 1.0$ ,  $Pr = 0.7$ , and inclination angles from  $0^\circ$  to  $60^\circ$ . The investigation showed that the mean Nusselt number decreases as the heated strip enlarges, and increases along with the inclination angle. Kent [6] used the finite volume method to study triangular enclosures for both summer and winter conditions within the range  $10^3 \leq Ra \leq 10^5$  for  $15^\circ \leq \theta \leq 75^\circ$ . It was observed that, for winter conditions and at small pitch angles, increasing  $Ra$  resulted into a multicellular flow structure. Further review on this subject can be found in Kamiyo et al. [7].

It is worthy of note that most of the studies on triangular enclosures have been restricted to isosceles or right-angled shapes. Reports on scalene shape are uncommon, despite that many buildings in different climes are of that shape. In this paper, ANSYS FLUENT<sup>®</sup>, a finite volume CFD package, is employed to study the flow field and heat transfer in rooftop-shaped asymmetric triangular cavities when heated from the base wall (winter condition). As in all the investigations mentioned previously, this study is restricted to steady laminar flow conditions ( $Ra \leq 5.25 \times 10^7$ ).

## 2. Computational details

A long air-filled ( $Pr = 0.71$ ) triangular enclosure with a triangular cross-section is considered as shown in Fig. 1. The enclosure extension in the direction perpendicular to the cross-section is assumed more than double its width so that the flow features can be assumed to be two-dimensional [8].

The horizontal base, depicting a ceiling being heated by the warm space below it, is assigned a uniform temperature  $T_H$ . The pitched roof is considered to be all at the same cold temperature,  $T_C$ . Four pitch angles,  $14^\circ$ ,  $25^\circ$ ,  $35^\circ$ , and  $45^\circ$ , representing an aspect ratio range  $0.2 \leq AR \leq 1.0$  were simulated. The enclosure aspect ratio,  $AR$ , is defined here as the ratio of the enclosure height,  $H$ , to the left fraction of the base,  $L_L$  (as from Fig. 1). The base length and the base length ratio,  $L_L/L_R$ , were kept unchanged in all the analysis. The Rayleigh and Prandtl numbers are defined

$$Ra = \frac{g\beta(T_H - T_C)H^3}{\nu\alpha} ; Pr = \frac{\nu}{\alpha}$$

Here,  $g$  is the gravitational acceleration module, and  $\alpha$ ,  $\beta$ , and  $\nu$ , designate the thermal diffusivity, the thermal expansion coefficient, and the kinematic viscosity of air, respectively.

Leaving the base-length unchanged, results in a progressive increase in the cavity height for increasing the pitch angle. This, in combination with a fixed temperature difference between the hot and cold walls, constrains the Rayleigh number to increase steadily with the pitch angle. In the four cases considered, the Rayleigh number ranges between  $8.06 \times 10^5$  and  $5.29 \times 10^7$ . The four geometries considered and the corresponding Ra-values are reported in Table 1.

PITCH ANGLE ( $\theta$ )	14°	25°	35°	45°
BASE LENGTH RATIO ( $L_L/L_R$ )	3:1	3:1	3:1	3:1
ASPECT RATIO ( $AR = H/L_L$ )	0.2	0.5	0.7	1.0
RAYLEIGH NUMBER (Ra)	$8.06 \times 10^5$	$5.27 \times 10^6$	$1.78 \times 10^7$	$5.29 \times 10^7$

**Table 1.** Non-dimensional characterization of the enclosures, and Rayleigh number values

The governing equations for buoyancy-driven laminar flow under steady-state conditions are conservation of mass, momentum and energy. Subject to the Boussinesq approximation, they are written

$$\begin{aligned}\frac{\partial u}{\partial x} + \frac{\partial v}{\partial y} &= 0 \\ \frac{u \partial u}{\partial x} + \frac{v \partial u}{\partial y} &= -\frac{1}{\rho} \frac{\partial p}{\partial x} + \nu \left( \frac{\partial^2 u}{\partial x^2} + \frac{\partial^2 u}{\partial y^2} \right) \\ \frac{u \partial v}{\partial x} + \frac{v \partial v}{\partial y} &= -\frac{1}{\rho} \frac{\partial p}{\partial y} + \nu \left( \frac{\partial^2 v}{\partial x^2} + \frac{\partial^2 v}{\partial y^2} \right) + g\beta(T - T_c) \\ \frac{u \partial T}{\partial x} + \frac{v \partial T}{\partial y} &= \alpha \left( \frac{\partial^2 T}{\partial x^2} + \frac{\partial^2 T}{\partial y^2} \right)\end{aligned}$$

Here,  $x$  and  $y$  designate the horizontal and vertical coordinates, and  $u$ ,  $v$ ,  $T$ ,  $p$  are the field variables: horizontal and vertical velocity components, temperature, and pressure.

The validity of the Boussinesq approximation in the present context is corroborated by Gray and Giorgini [9], since they reported that the results would deviate of at most 3% from the corresponding non-Boussinesq solution. Also, in the process of validating their code, Ridouane et al. [10] re-examined the benchmark numerical study of natural convection of air in a square enclosure carried out by de Vahl Davis [11]. Results obtained without enforcing the Boussinesq approximation were just 2% different from the benchmark solution. Such a level of accuracy is generally considered to be acceptable for natural convection flow simulations.

The computational domain coincides with the physical domain. The triangular shape of the domain makes it difficult to use a structured grid; use was therefore made of unstructured triangular meshes.

The steady-state flow field and heat transfer predictions were carried out using the finite volume based ANSYS FLUENT<sup>®</sup> code (version 14). The SIMPLE algorithm was employed for solving the pressure and velocity coupling, while the PRESTO discretization scheme was enforced for pressure. The QUICK scheme was adopted for space discretization of the momentum and energy equations. The use of the above schemes, combined with body-fitted meshes having the corners inflated with nodes tightly clustered, is expected to guarantee good accuracy in the prediction of the local and mean Nusselt numbers. About  $10^4$  grid elements were used for the final simulations, after a series of grid-

independence experiments. For example, results were obtained for 6344, 9196 and 12,438 elements, for the 14°-pitch triangle. For the sake of exemplification, the grid for case  $\theta = 35^\circ$  is shown in Fig. 2. Convergence criteria were fixed at  $5 \times 10^{-6}$  for the continuity residual, and at  $10^{-7}$  for the residuals of the momentum and energy equations.

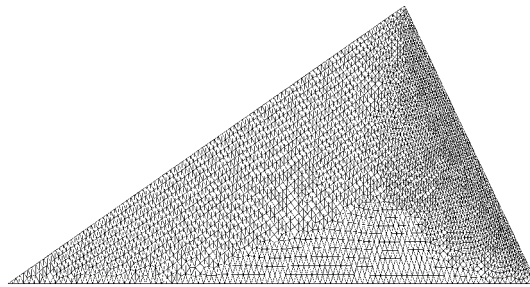


**Figure 2.** Computational grid for the 35°-pitch triangle.

### 3. Results and discussion

Results are given in terms of streamline and isotherm representations in Figs. 3 and 4, respectively. The stream-function is scaled using  $U = \sqrt{g\beta(T_H - T_C)H}$  as the reference velocity, and  $H$  as the scale length. Isotherms are for the non-dimensional temperature  $\Theta = (T - T_C)/(T_H - T_C)$  and, therefore, range from zero to one. The x-coordinate is scaled with the base length,  $L$ , with the origin in correspondence of the triangle vertex ( $-0.75 \leq x/L \leq +0.25$ ).

The results in Fig. 2 show that, over the relatively high Ra-range covered by this numerical experiment, the flow is always characterized by the presence of multiple buoyancy-driven vortices. Fig. 3, correspondingly, demonstrates that the thermal field is convection-dominated even at the lowest Ra-value, with no evidence of thermal diffusion. In all the cases the flow-field is led by a main central vortex rotating clockwise with a relatively high velocity. This drives smaller counter-rotating cells, whose number and strength changes drastically as the pitch angle increases. Up to ten vortices, whose size progressively reduces towards the lower corners, can be observed in the shallow 14°-pitch cavity (Fig. 2.a). These reduce to two large cells and three smaller vortices for the 25°-pitch enclosure. The vortex structure remains similar for the 35°-pitch enclosure, where, however, a single vortex resists at the left lower corner, while two rolls appear at the upper corner. In the 45°-pitch enclosure (Fig. 2.d), the two large counter-rotating cells observed in (Fig. 2.c) merge to form a larger vortex occupying the lower part of the space, while smaller cells are formed towards the top and bottom-left corners. It is observed that the multi-cellular flow structure is now vertical, as opposite to the one observed for the lowest pitch-value. In each enclosure, the velocity of rotation decreases as the cell size reduces.

This result is similar to that of Holtzman et al. [12] who presented flow visualization results from experiments performed in a smoke-filled isosceles triangular enclosure heated from the base wall, to show that, as Ra increases for a given geometry, the flow pattern becomes multi-cellular and the number of counter-rotating cells increases.

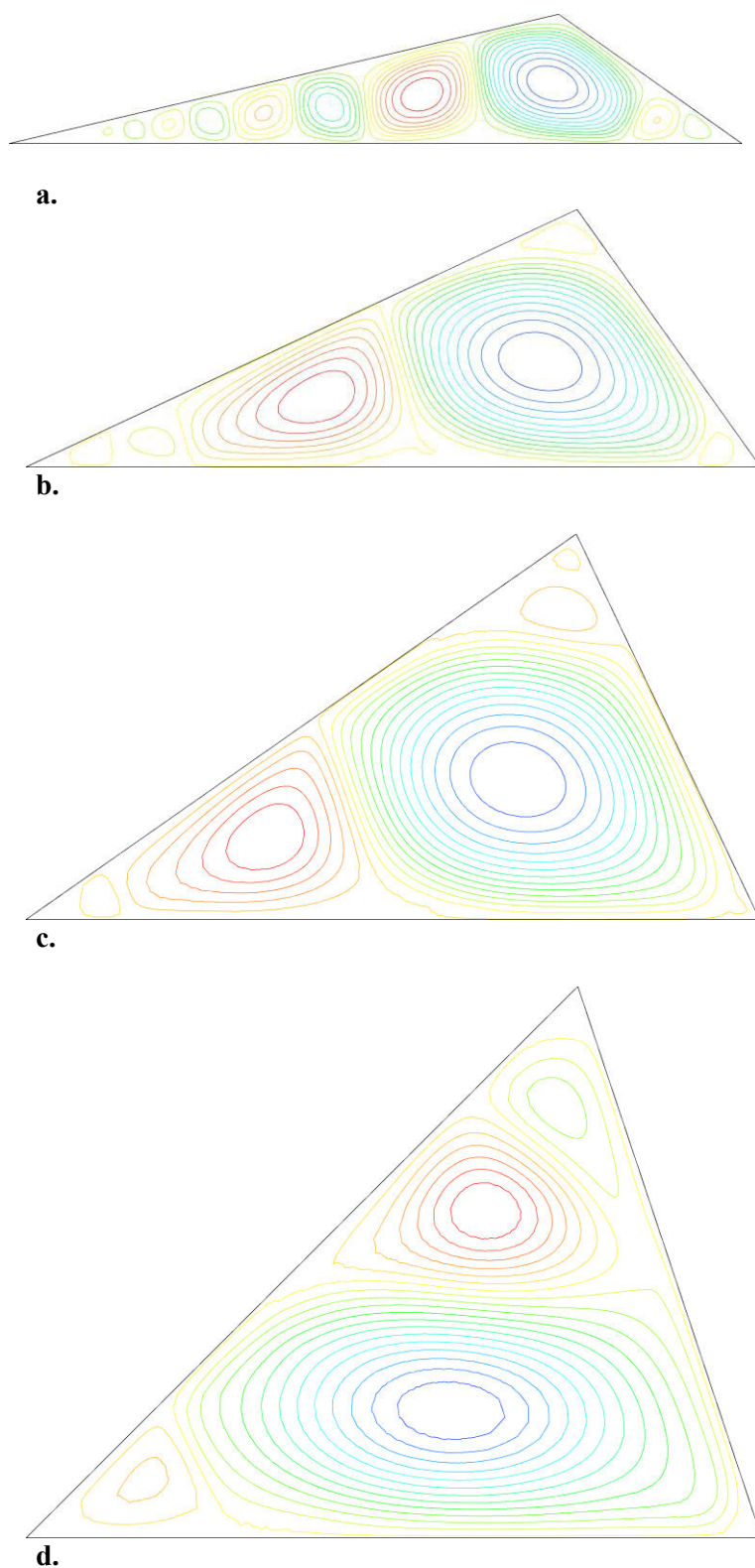


**Figure 3.** Streamlines – colors indicate the strength of the circulations (clockwise from blue to yellow – Counterclockwise from orange to red) – a.  $\theta = 14^\circ$ ; b.  $\theta = 25^\circ$ ; c.  $\theta = 35^\circ$ ; d.  $\theta = 45^\circ$ .

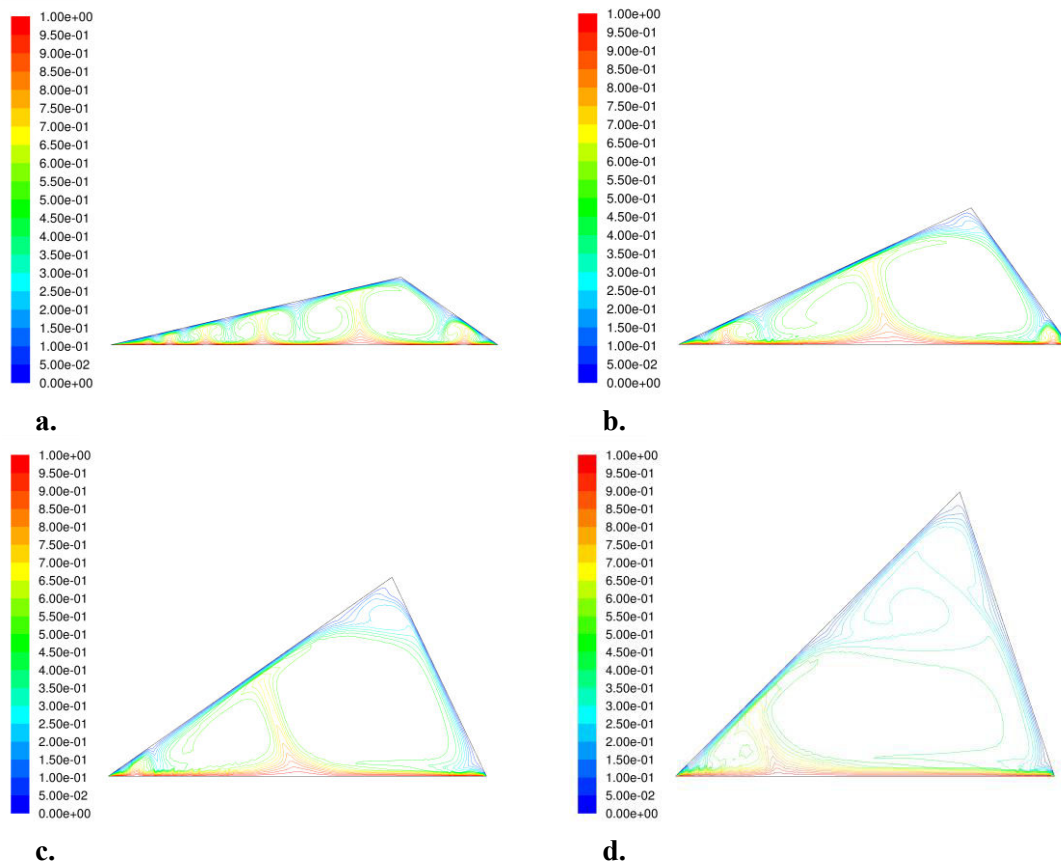


**Figure 3.** Isotherms  $\Theta = (T - T_C) / (T_H - T_C)$  – a.  $\theta = 14^\circ$ ; b.  $\theta = 25^\circ$ ; c.  $\theta = 35^\circ$ ; d.  $\theta = 45^\circ$ .

The strength and number of the vortices definitely controls the transport processes within the enclosures, as confirmed by the thermal fields in Fig. 3. Isotherms indicate the presence of hot thermal plumes rising from the base side and of cold jets leaving the cold upper sides. These correspond to regions included between two counter-rotating rolls, where the convective transport attains its maximum efficiency. As a consequence, the number of thermals progressively reduces for increasing the pitch angle. The multi-cellular flow within the  $14^\circ$ -pitch enclosure, Fig. 3.a, results in a thorough mixing of the fluid, to which corresponds a relatively high value of the mean temperature of air. In addition, high temperature gradients are observed at the periphery of the cells and along the walls. The temperature distribution within the enclosure becomes progressively more uniform as the aspect ratio and the Rayleigh number increase. This effect is directly related to the formation of big vortices whose central part remains practically isothermal and at temperatures of order 0.3-0.4.

The local values of the heat transfer coefficient,  $h_x$ , are reported in Fig. 4, in terms of the local Nusselt number

$$Nu_{x,L} = \frac{h_x L}{\lambda}$$

where  $\lambda$  is the thermal conductivity of air. In the Nusselt number definition, the base length,  $L$ , was preferred to the cavity height,  $H$ , to facilitate the direct comparison of results relevant to different geometries, but having a common base-length. In Fig. 4, data for the hot and cold walls are both referred to the  $x$ -coordinate.

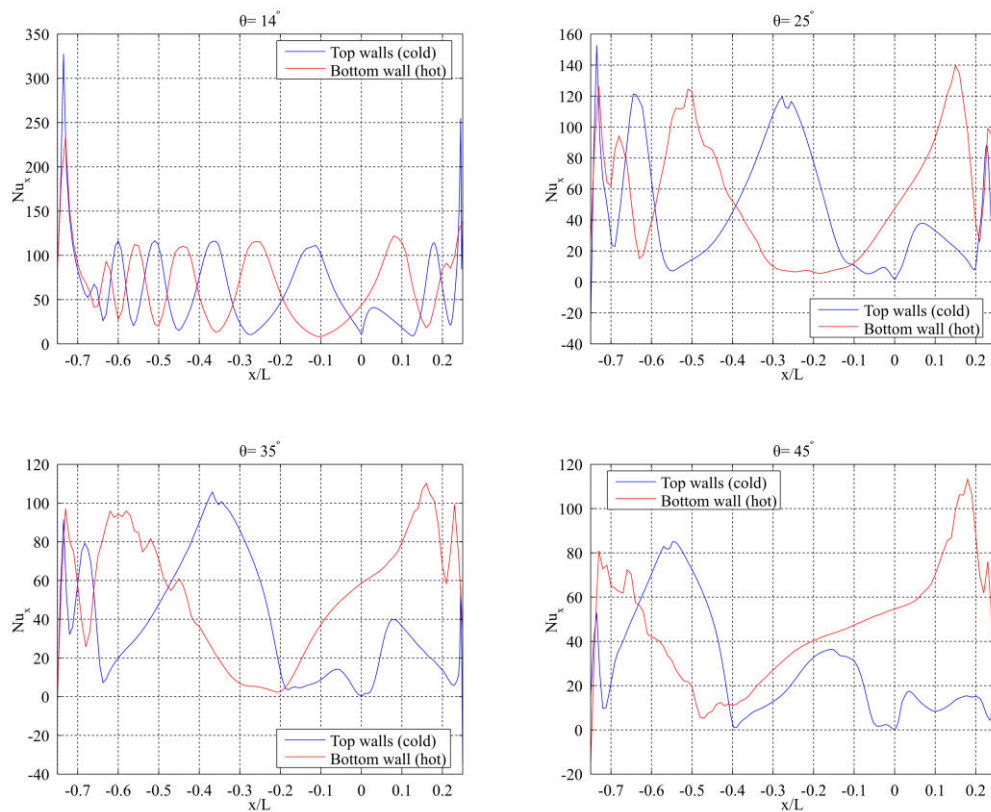


**Figure 4.** Local Nusselt number distributions along the bottom (red), and top (blue) enclosure walls.

The Nusselt number distributions along the bottom and top surfaces confirm that the heat transfer rate is directly linked to the attachment and detachment processes of the thermal plumes at the solid walls. In particular, as expected, maxima and minima in  $Nu_{x,L}$  closely correspond to thermal-jet impact points, and to detachment saddle points, respectively. This is particularly well evident for the 14°-pitch in Fig. 4, showing a quite well ordered oscillatory sequence. This is no longer the case for the highest pitch-angle values, 35° and 45°, where the trends become irregular and a limited number of relatively high peak-value is observed. A minimum in  $Nu_{x,L}$  is always found at the upper corner, since air stagnates in its correspondence. The heat transfer rate drops to zero, or quasi-zero, at the detachment points, where air at the wall temperature is driven on the separation area by two counter-rotating vortices, thus creating a region of almost-zero temperature gradient over it. In most of the cases high Nu-values are found in the vicinity of the bottom corners, mainly due to the closeness of the hot and cold walls. These extreme values are however of little practical significance in terms of the overall heat transfer efficiency of the system. This is well documented by the values of the mean Nusselt number over the bottom wall in Fig.5. Results are presented for two alternative Nusselt number definitions, assuming the base length,  $L$ , and the cavity height,  $H$ , as the reference length, respectively

$$Nu_{av,L} = \frac{h_{av}L}{\lambda} ; \quad Nu_{av,H} = \frac{h_{av}H}{\lambda}$$



Here,  $h_{av}$  is the mean value of  $h_x$  over  $L$ . While it is obvious that the two definitions are equivalent, they have different informative contents in terms of interpretation of the heat transfer results.

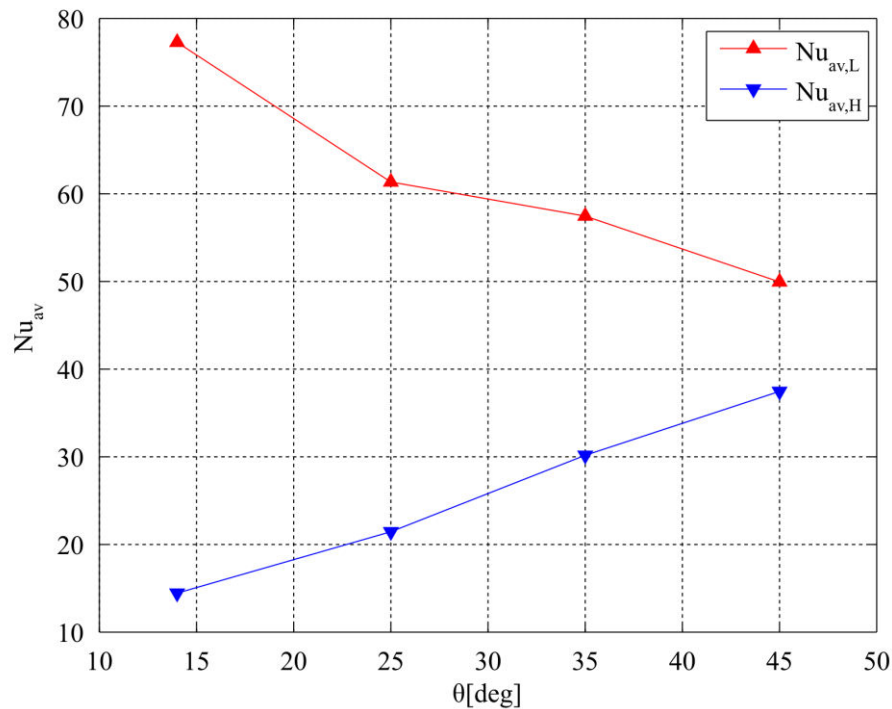


**Figure 5.** Averaged Nusselt-number values for the bottom enclosure wall.

The increasing trend of  $Nu_{av,H}$  with  $\theta$  actually corresponds to expectations, since  $Ra$  changes of two orders of magnitude passing from the  $14^\circ$  to the  $45^\circ$ -pitch angle cases. The  $Nu_{av,H} - \theta$  plot is quasi-linear, and this results in an almost linear dependence of  $Nu_{av,H}$  on  $Ra^{1/3}$ . However, the increasing trend of  $Nu_{av,H}$  with the Rayleigh number might lead to the wrong conclusion that the system's heat transfer efficiency increases for increasing  $\theta$ . That this is actually not the case is clearly shown by the decreasing trend of  $Nu_{av,L}$ . This parameter directly reflects the total heat transfer rate, and, for cases of equal base-length, indicates that the thermal power driven to the cold walls undergoes a 23% reduction passing from the  $14^\circ$ - to the  $25^\circ$ -pitch case, reducing further for increasing  $\theta$ .

The practical significance of the above results is that the reduction of the number of the buoyancy-driven rolls and their progressive vertical alignment for increasing the pitch-angle provide a corresponding reduction of the heat transfer rate, in spite of the increase in the buoyancy forces indicated by the Rayleigh number.

#### 4. Conclusion

Two-dimensional, steady, laminar natural convection of air contained in a long, horizontal asymmetric triangular enclosure was investigated for bottom heating conditions, while varying the pitch-angle and keeping unchanged the enclosure base-length and the upper vertex coordinate. The results show that, over the range covered by the numerical experiment, heat is transferred from the hot base wall to the cold inclined walls by a multi-cellular flow structure. As the pitch angle increases, the number of cells is seen to reduce, and the cells tend to pass from a horizontal alignment to a vertical one. Since the Rayleigh number increases with the third power of the enclosure height, it would be expected that the higher the pitch angle is the higher is the heat transfer rate. Results however demonstrate that the effect of the pitch angle is just the opposite, since, in fact, the above-mentioned reorganization of the



buoyancy-driven circulations invariably produces a reduction in the heat transfer coefficients for increasing  $\theta$ . The work therefore provides qualitative directions for the choice of a roof shape, in view of the control of heat losses through triangular attic spaces.

## References

- [1] ASHRAE Handbook: Fundamentals 2005, SI Edition, ASHRAE Inc., USA
- [2] Gershuni GZ, Zhukhovitskiy EM and Shvartzblat, DL 1974 *Hydrodyn.* **7** 89
- [3] Poulidakos D and Bejan A 1983 *J. Heat Transfer* **105** 652
- [4] Ridouane EH and Campo A 2006 *Proc. 9th AIAA/ASME Joint Thermophysics Heat Transfer Conference*, California.
- [5] Sahar G, Tofiqul I, Saha S and Quamrul I 2007 *Thammasat Int. J. Sci. and Tech.* **12** 24
- [6] Kent EF 2009 *Proc. IMechE C* **223** 1157
- [7] Kamiyo OM, Angeli D, Barozzi GS, Collins MW, Olunloyo VOS and Talabi SO 2010 *Appl. Mech. Rev.* **63**
- [8] Penot F and N'Dame A 1992 *Proc 3rd UK National Conf. and 1st European Conf. on Thermal Science*, Birmingham, UK
- [9] Gray DD and Giorgini A 1976 *Int. J. Heat Mass Transfer* **19** 545
- [10] Ridouane EH, Campo A and McGarry M 2005 *Int. J. Thermal Sci.* **44** 944
- [11] De Vahl Davis G 1983 *Int. J. Num. Meth. Fluids* **3** 249
- [12] Holtzman GA, Hill, RW and Ball, KS 2000 *J. Heat Transfer* **122** 485

*In memory of*

**Prof. Michael Wesley Collins**



This short commemoration is dedicated to Prof. Michael W. Collins, as an outstanding researcher in thermal sciences, a passionate promoter of education in sciences, and a very good friend of Italy and UIT (Italian Union of Thermo-Fluid Dynamics).

Michael left us on 2014 August 23<sup>rd</sup>, after a short, but relentless disease. He had been born in Dorchester, Dorset, UK, in 1939. He got the BA in Engineering Science at the University of Oxford, and run most of his academic career at City University, in London, where he served as Lecturer, Senior Lecturer, and Professor, up to his retirement in 1998. At City University he first got the Ph.D. in Mechanical Engineering, and the title of Doctor of Science in 1990.

Besides, Michael Collins was Visiting Professor at Fudan University, Shanghai & Shanghai University of Science & Technology, at London South Bank University, and at Brunel University, West London, from 2005.

He was appointed Honorary Fellow of UIT in 1991 and Copernicus Visiting Scientist at the University of Ferrara, Italy, in 2006. He was awarded the Knights Cross, Order of Merit for services to Polish Science, in 1991, and the Busk Prize of the Royal Aeronautical Society in 1992.

The above public recognitions of the scientific value of Michael Collins are the results of his untiring research activity, resulting in an incredible number of scientific contributions, around 400, including papers in archival journals, conference keynotes and papers, contributions to volumes.

Heat transfer by convection was his first, and never abandoned, field of interest, even if his open minded view of science led him soon to extend his studies to other bordering topics, such as computational thermofluids, applied mathematics (Michel was Chartered Mathematician as well as Chartered Engineer), medical flows, non-invasive measurement methods and data processing, joint engineering & biological studies.

Michael Collins collaboration with the Italian heat transfer community dates back to 1983, when he was appointed Contract Professor at University of Bologna, and did never interrupt up to his death. We remember him as a member of the Scientific Committee and as an invited speaker in several UIT Conferences, as well as the supervisor of a number of Italian Ph.D. students. Under this latter aspect, the role of Michael Collins in indicating novel and frontier research topics to our scientific community deserves special mention.

*Giovanni Sebastiano Barozzi and Walter Grassi*